Thermochimica Acta 472 (2008) 64–73

Contents lists available at ScienceDirect

Thermochimica Acta

journal homepage: www.elsevier.com/locate/tca

Hydration characteristics and hydration products of tricalcium silicate doped with a combination of MgO, Al_2O_3 and Fe_2O_3

Dietmar Stephan[a,*,1], Sophie Njooh Dikoundou[c,1], Gabriele Raudaschl-Sieber[b]

[a] Universität Kassel, Institut für Konstruktiven Ingenieurbau, Mönchebergstraße 7, 34125 Kassel, Germany
[b] Technische Universität München, Anorganische Chemie, Lichtenbergstraße 4, 85747 Garching, Germany
[c] Verein Deutscher Zementwerke e.V., Forschungsinstitut der Zementindustrie, Tannenstraße 2, 40476 Düsseldorf, Germany

ARTICLE INFO

Article history:
Received 7 March 2007
Received in revised form 16 March 2008
Accepted 18 March 2008
Available online 29 March 2008

Keywords:
Tricalcium silicate
Foreign oxides
Heat of hydration
Isothermal conduction calorimetry
^{29}Si nuclear magnetic resonance

ABSTRACT

Tricalcium silicate is the major component of ordinary Portland cement and the hydration products are responsible for the high strength of cementitious products. It is known that the crystal structure of tricalcium silicate depends on the kind and amount of foreign oxides incorporated into the lattice. In this study the influence of multiple doping with MgO, Al_2O_3 and Fe_2O_3 on the hydration characteristics was analysed by isothermal heat-conduction calorimetry. The hydration products were characterised by differential scanning calorimetry, X-ray diffraction, ^{29}Si solid-state nuclear magnetic resonance spectroscopy and scanning electron microscopy. The hydration is dominated by the kind and concentration of foreign oxides, independent of the influence of the doped oxide on the crystal structure of C_3S. Combined doping with MgO + Al_2O_3 or MgO + Fe_2O_3 shows no interactions between the foreign oxides on their influence on hydration. In the case of combined doping with Al_2O_3 + Fe_2O_3, the retarding effect of Fe_2O_3 on the main reaction is much stronger in the presence of Al_2O_3.

1. Introduction

The major component of ordinary Portland cement (OPC) is a 50–75 wt.% solid solution of tricalcium silicate ($3CaO{\cdot}SiO_2 = C_3S$[2]) with MgO, Al_2O_3 and Fe_2O_3 [1–4]. The solid solution is called alite and the hydration products are responsible for the high strength of hydrated OPC. Former studies [5–7] show that foreign oxides not only affect the crystal structure of C_3S and C_3A ($3CaO{\cdot}Al_2O_3$) but also their hydration characteristics. The hydration characteristic is essential for the performance of OPC and can be monitored by isothermal calorimetry. The purpose of this study is a better understanding of the effect of impurities in tricalcium silicate on its hydration characteristics.

Besides the well-known application of alite as the main phase in OPC, several recent studies showed that different calcium silicate ceramics have excellent bioactivity when immersed in simulated body fluid (SBF). Tricalcium silicate can induce apatite formation when soaked in SBF and therefore is a potential candidate for new biomaterials for hard tissue repair. Examples for bioactive ceramics based on calcium silicate are wollastonite and pseudowollastonite [8,9] as well as dicalcium silicate [10,11] and tricalcium silicate [12,13]. Most likely, foreign ions can also modify the material properties of C_3S based biocompatible ceramics as implant material for clinical applications.

The aim of the this study was to learn more about the influence of combined doping of C_3S with MgO, Al_2O_3 and FeO_3 on the synthesis, grindability and lattice parameters of the clinker phase and the influence of these metal oxides on the hydration kinetics and hydration products.

1.1. C_3S hydration

At ambient conditions, tricalcium silicate reacts with water in an exothermic reaction to form calcium silicate hydrate with lower calcium content than the starting material and portlandite (CH) as a side product. Calcium silicate hydrate is an apparently amorphous phase of variable composition, and hence is expressed as C–S–H, which implies a non-stoichiometric composition. The hydration can be expressed in a general equation [14]:

$$3CaO{\cdot}SiO_2 + xH_2O \rightarrow yCaO{\cdot}SiO_2{\cdot}(y-(3-x))H_2O + (3-y)Ca(OH)_2$$

The composition of C–S–H depends on the hydration conditions, e.g. temperature and water/solid-ratio. C–S–H is probably a metastable product in most cases, but at a water/solid-ratio of 0.45,

* Corresponding author at: Universität Kassel, Institut für Konstruktiven Ingenieurbau, Mönchebergstraße 7, 34125 Kassel, Germany. Tel.: +49 561 804 2603; fax: +49 561 804 2662.
E-mail address: dietmar.stephan@uni-kassel.de (D. Stephan).

[1] Former position at TUM.

[2] Abbreviation in cement chemistry: CaO=C, SiO_2=S, Al_2O_3=A, Fe_2O_3=F, MgO=M, H_2O=H.

0040-6031/$ – see front matter © 2008 Elsevier B.V. All rights reserved.
doi:10.1016/j.tca.2008.03.013

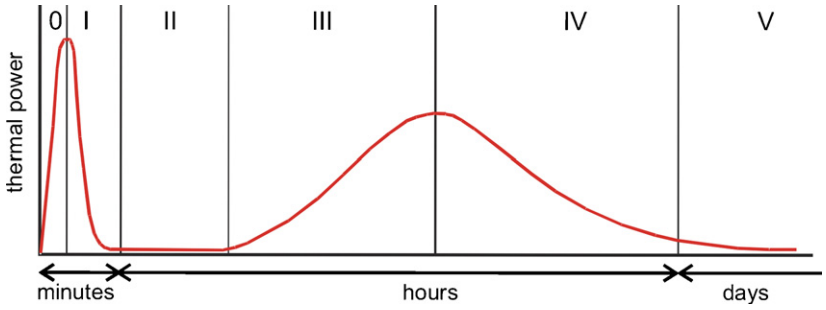

Fig. 1. Schematic changes taking place during isothermal calorimetry, after Gartner et al. [16].

crystalline afwillite ($C_3S_2H_3$) may be the thermodynamically stable product at room temperature [15].

Schematic illustration of the changes taking place during isothermal calorimetry is shown in Fig. 1. Soon after the first wetting, an initial rapid exothermic reaction (stage 0) appears due to a surface hydrolysis and the release of ions into solution. This is followed by deceleration of the heat evolution (stage I) caused by the formation of metastable calcium silicate hydrate [C–S–H (m)] on the surface of C_3S and retarded dissolution. The induction period (stage II) is characterised by an increasing supersaturation with respect to $Ca(OH)_2$ and retarded nucleation of final products. The time at which the maximum supersaturation is reached before $Ca(OH)_2$ begins to crystallise at a significant rate, strongly depends on the reactivity of C_3S and the water/solid-ratio. In the beginning of the acceleration period (stage III) nucleation of a more stable form of C–S–H [C–S–H (s)] is observed together with a decrease of the concentration of Ca^{2+} in solution. Once the C–S–H (s) has nucleated, growth of the new phase occurs at the expense of C–S–H (m) and the setting of the C_3S lime takes place. During the second deceleration period (stage IV) the growth of hydration products continues into empty spaces and is followed by the final slow reaction (stage V) with a gradual densification of the microstructure, recrystallisation of $Ca(OH)_2$ associated with a continued hardening [16].

If C_3S is hydrated at ambient conditions, the C–S–H phases are X-ray amorphous and X-ray diffraction methods show only the decrease of the crystalline C_3S and the increase of the side product $Ca(OH)_2$. 1.4 nm tobermorite and jennite can be taken into account as idealised chemical structure for C–S–H with different amounts of water and ratios of Ca/Si [17]. For this X-ray amorphous product, ^{29}Si solid-state NMR is an ideal tool to get more structural information. NMR is most sensitive to local ordering and structure around the spin nucleons and permits structural studies not only of crystalline materials but also of poorly crystalline and amorphous materials [18]. With NMR it is possible to distinguish how many other Si atoms (n) are bonded to a central Si atom (Q^n, $n = 0$, 1, 2, 3 and 4). Fig. 2 gives an example for the 1.4 nm tobermorite with Si in different positions. For the incorporation of foreign oxides into C–S–H Richardson and Groves [19] and Andersen et al. [20] demonstrated that it is also possible to distinguish between Si bonded to two other Si atoms and Si bonded to Al incorporated into the C–S–H structure.

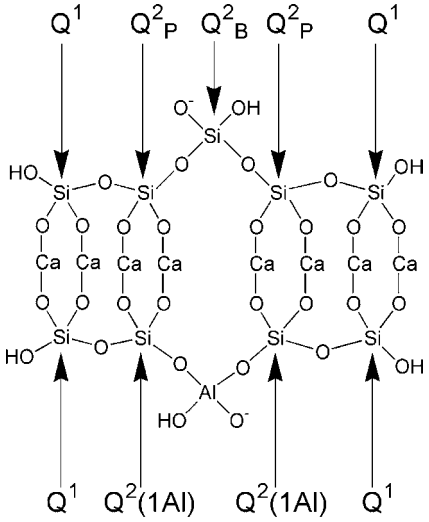

Fig. 2. Representation of single layer in the crystal structure of 1.4 nm tobermorite; the upper part shows characteristic features for the "dreierkette"-based models for the C–S–H phase, the lower part illustrates the incorporation of Al in the bridging side of the silicate chain (after [20]); Q^1: one Si is bonded via an oxygen bond; Q^2: two Si are bonded via oxygen bonds; B means "bridging" and P means "paired" silicon tetrahedra.

1.2. Results of preceding studies

Many samples of tricalcium silicate doped with different amounts of MgO, Al_2O_3 and Fe_2O_3 were synthesised using an innovative sol–gel process as precursor [21]. The doping with foreign oxides had a strong influence on the sintering, grindability and coloured appearance of C_3S. The sintering of the samples increased with higher concentrations of doped foreign oxides and went hand in hand with continual shrinkage. Grindability was not influenced by MgO but grindability was worsened by Fe_2O_3 and even more by Al_2O_3. Changes in colour gave visible indication that combined doping has another influence compared to doping with only one foreign oxide. Structural changes of C_3S were qualitatively monitored by X-ray powder diffraction and could be quantified by changes in the lattice parameters after performing Rietveld refinement. Single doping of MgO or Al_2O_3 significantly altered the crystal structure of C_3S, whereas the influence of Fe_2O_3 was almost insignificant. With respect to the lattice parameters, the effect of combined doping with MgO + Al_2O_3 is additive, but structural changes decrease with the total amount of foreign oxides in the sample. Structural changes initiated by the addition of Fe_2O_3 were much stronger when MgO and/or Al_2O_3 were present than with Fe_2O_3 alone. ^{29}Si MAS NMR showed that Fe_2O_3 and Al_2O_3 had a significant influence on the local ordering of Si in C_3S. More details about the influence of combined doping with MgO, Al_2O_3 and Fe_2O_3 can be found in a recent publication [22].

In the present study the hydration characteristic and hydration products of combined doped tricalcium silicate are highlighted.

Table 1
Concentration of doped foreign oxides and sample abbreviation

	Foreign oxide	Abbreviation	Concentration of MgO in wt.%	Concentration of Al_2O_3 in wt.%	Concentration of Fe_2O_3 in wt.%
Undoped	Reference	R = M0A0F0	0	–	–
Doped with one metal oxide	MgO	M1	0.33	–	–
		M2	0.66		
		M3	1.33		
		M4	2.00		
	Al_2O_3	A1	–	0.50	–
		A2		1.00	
	Fe_2O_3	F1	–	–	0.37
		F2			0.73
		F3			1.10
	$MgO + Al_2O_3$	M1A1	0.33	0.50	–
		M1A1		1.00	
		M2A1	0.66	0.50	
		M2A2		1.00	
		M3A1	1.33	0.50	
		M3A2		1.00	
		M4A1	2.00	0.50	
		M4A2		1.00	
Doped with two metal oxides	$MgO + Fe_2O_3$	M1F1	0.33	–	0.37
		M1F2			0.73
		M1F3			1.10
		M2F1	0.66		0.37
		M2F2			0.73
		M2F3			1.10
		M3F1	1.33		0.37
		M3F2			0.73
		M3F3			1.10
		M4F1	2.00		0.37
		M4F2			0.73
		M4F3			1.10
	$Al_2O_3 + Fe_2O_3$	A1F1	–	0.50	0.37
		A1F2			0.73
		A1F3			1.10
		A2F1		1.00	0.37
		A2F2			0.73
		A2F3			1.10
Doped with three metal oxides	$MgO + Al_2O_3 + Fe_2O_3$	M2A1F1	0.66	0.50	0.37
		M2A1F2			0.73
		M2A1F3			1.10
		M2A2F1		1.00	0.37
		M2A2F2			0.73
		M2A2F3			1.10
		M4A1F1	2.00	0.50	0.37
		M4A1F2			0.73
		M4A1F3			1.10
		M4A2F1		1.00	0.37
		M4A2F2			0.73
		M4A2F3			1.10

2. Experimental

The preparation and characterisation of the pure and doped C_3S is described in detail in [22]. Because the reactivity of C_3S depends on particle size, all samples were ground in a planetary ball mill (pulverisette 6, Fritsch, Idar-Oberstein, Germany) to the same fineness of $D_{50} = 5.3 \pm 0.5$ μm according to laser light scattering (CILAS 1064 LD, CILAS, Orleans, France). Table 1 gives the composition and sample abbreviation of the investigated samples.

The method used to characterise the hydration of C_3S was isothermal heat-conduction calorimetry (TAM air, Thermometric, Järfälla, Sweden). The heat evolution of samples with water/solid-ratio of 0.5 was investigated at 20 ± 0.1 °C. C_3S and water were tempered for several hours before the reaction was initiated by injecting the water into the reaction vessel and stirring the sample in the calorimeter for several minutes. This procedure allowed monitoring the heat evolution from the very beginning when water was added to the sample. Data logging was continued for nearly 7 days.

X-ray diffraction (XRD) patterns were measured with a D8 Advance (Bruker axs, Karlsruhe, Germany). Differential scanning calorimetry (DSC) was done with an STA 409 (Netzsch Gerätebau, Selb, Germany) at a heating rate of 10 K min^{-1}. ^{29}Si solid-state NMR experiments were performed on a Bruker Avance 300 (7.0445 T, 59.63 MHz) using a MAS probe for 7 mm zirconia rotors, a spinning speed of 5 kHz, single pulse excitation with a pulse width of 4 μs, a relaxation delay of 15 s and 1000–5000 scans. Chemical shifts refer to tetramethylsilane as an external

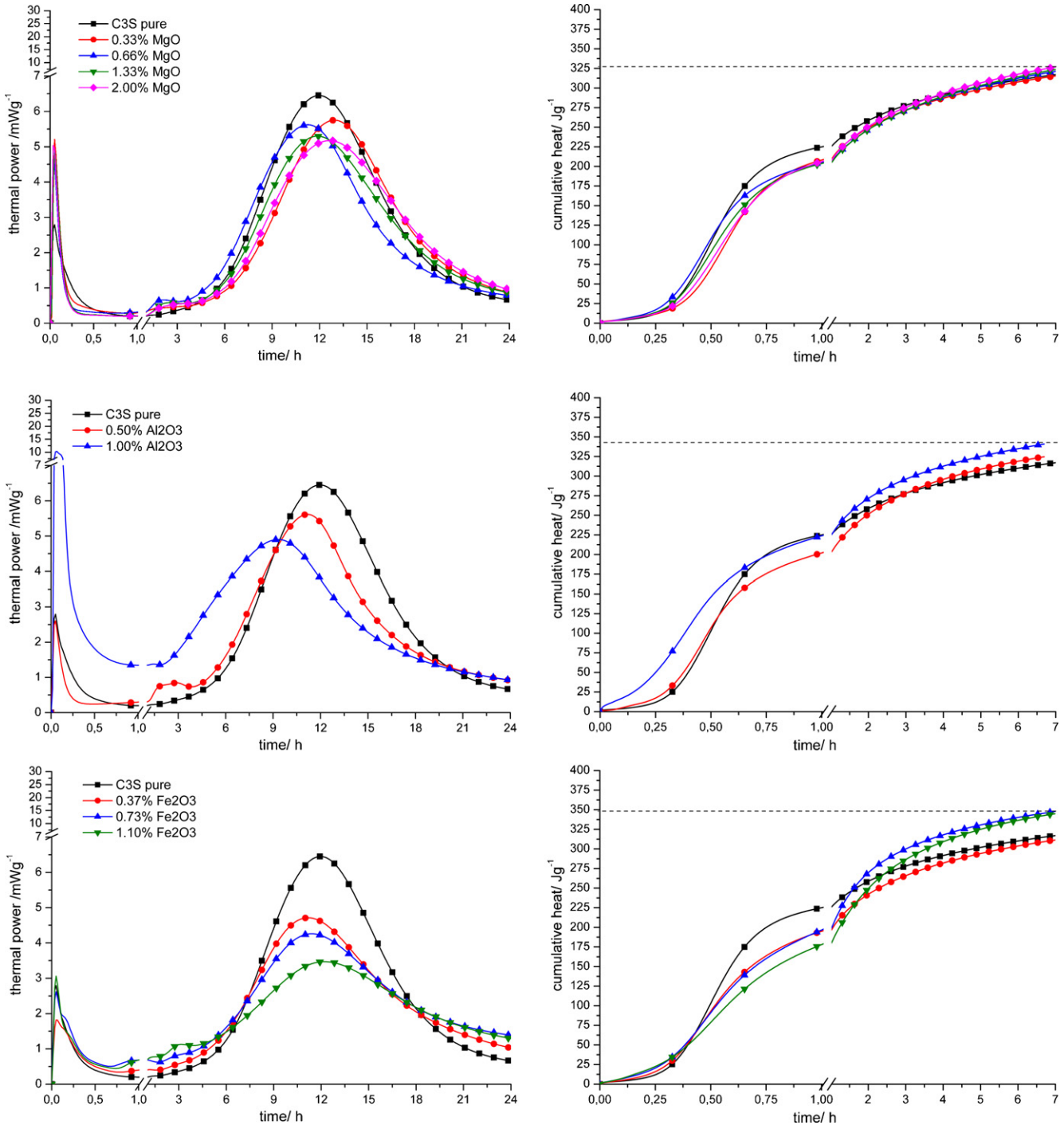

Fig. 3. Thermal power and cumulative heat of hydration of pure C_3S and single doped C_3S.

standard. Deconvolution of the peaks was performed with the least-squares fitting routine of OriginPro 8 (OriginLab Corporation).

3. Results and discussion

3.1. Heat of hydration

Heat evolution during the first 24 h of hydration is shown together with the cumulative heat of hydration over a period of 7 days for a selection of samples in Figs. 3 and 4. The results for doped samples are discussed in detail below.

3.2. Single doped C_3S

The effect of MgO on the hydration behaviour is least significant (Fig. 3a). The cumulative heat of hydration shows that MgO slows down the hydration of C_3S slightly during the first 24 h, but the overall heat of hydration is nearly the same after 7 days. This is in agreement with the results of Abdul-Maula and Odler [23].

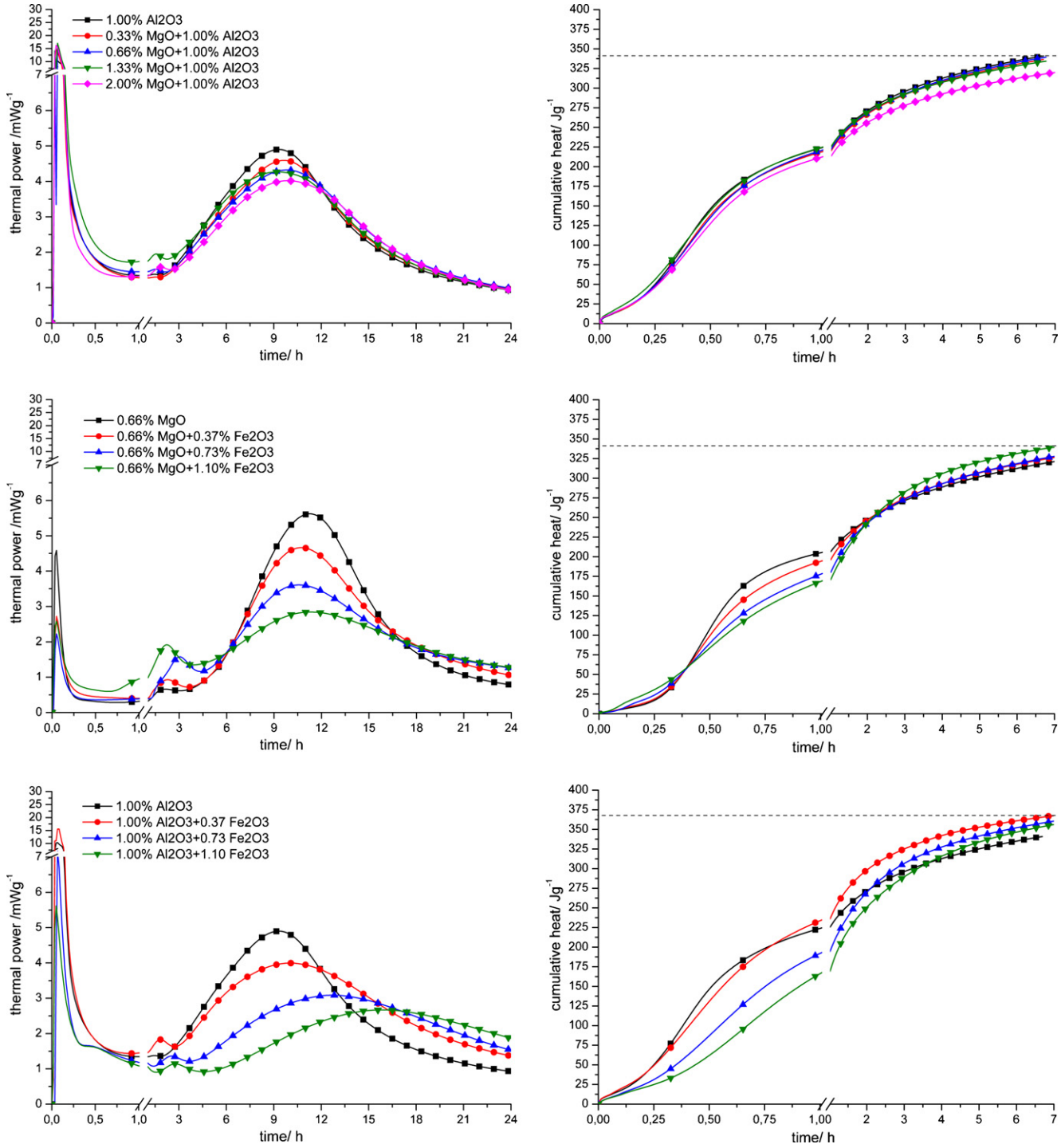

Fig. 4. Thermal power and cumulative heat of hydration of different samples.

Doping with Al_2O_3 dramatically intensifies the initial reaction due to increased surface hydrolysis. For these samples, heat evolution during the induction period is higher than for samples without Al_2O_3 and at the same time the intensity of the 2nd maximum decreases. After 7 days all doped samples again developed higher cumulative heat of hydration compared to pure C_3S (Fig. 3b).

No influence on the initial reaction is visible for the doping of C_3S with Fe_2O_3, but the main hydration peak is broader and significantly lower in intensity (Fig. 3c). This broader and lower main peak results in a little higher cumulative heat of hydration during the first 9 h, much lower cumulative heat after 1 day but after 7 days the cumulative heat of nearly all doped samples is distinctively higher than for the undoped one. This result is in line with the results published by Valenti et al. [24] and Fierens et al. [25].

A summary of the most characteristic data of all 48 different samples is given in Figs. 5–7. Data for samples with 0.33 and 1.33 wt.% MgO were skipped for clear arrangement.

3.3. *Multiple doped C_3S*

The investigation of samples doped with two or three foreign oxides shown in most cases the effect of the incorporated foreign

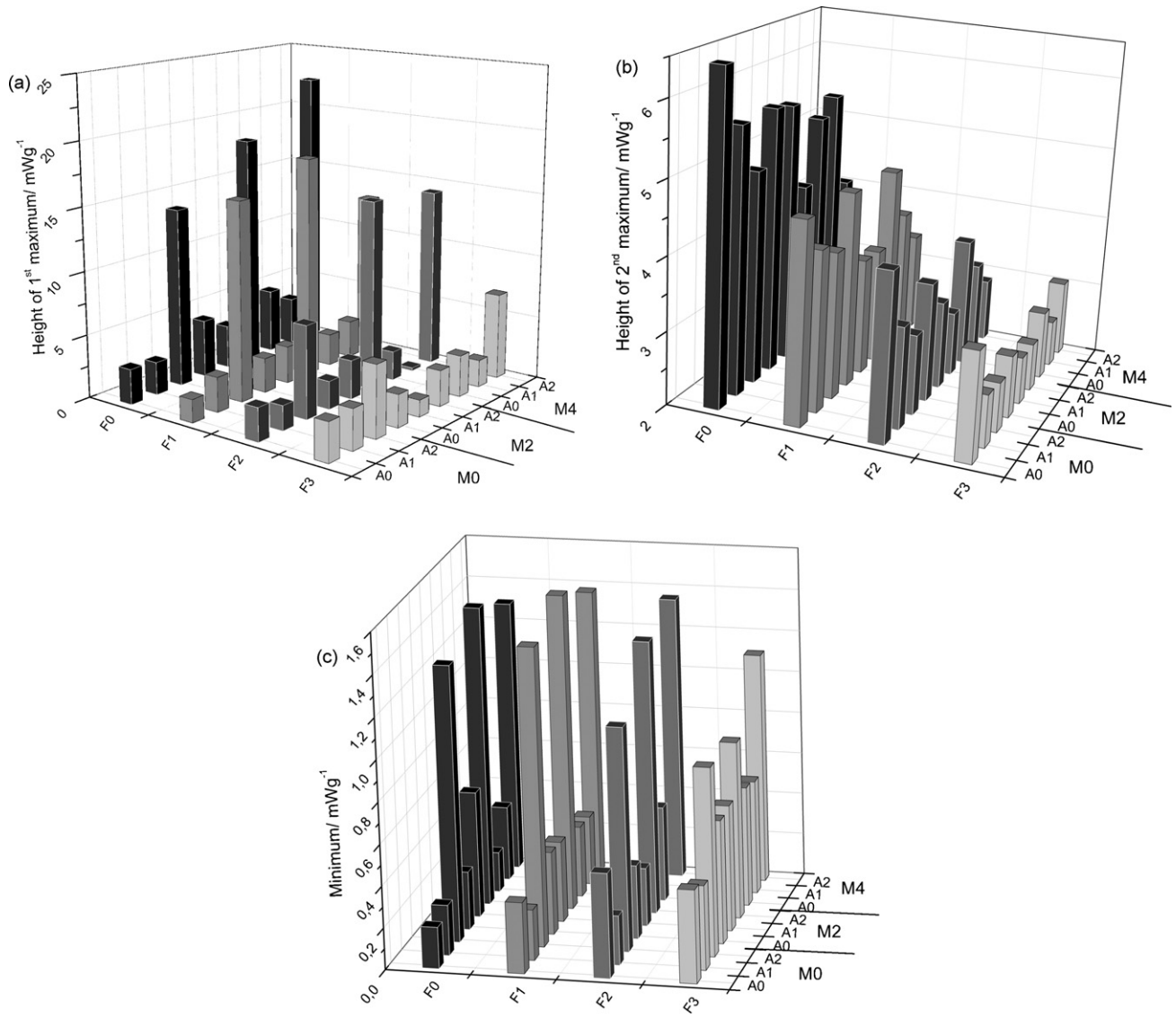

Fig. 5. Height of 1st and 2nd maxima (a and b) as well as minimum during the induction period (c).

oxides is additive. With some combinations, there is mutual interference of the oxides on the hydration characteristics.

Fig. 4 shows that doping with different amounts of MgO has almost no influence on the hydration characteristics of samples either doped with Al_2O_3 or Fe_2O_3. With all these combinations, the hydration is either dominated by Al_2O_3 or Fe_2O_3.

Samples doped with $Al_2O_3 + Fe_2O_3$ (Fig. 4c) are compared with samples doped only with Fe_2O_3 in Fig. 3c or $MgO + Fe_2O_3$ in Fig. 4b. Distinct differences in the hydration characteristics are visible. The very strong initial reaction caused by the doping with 1.0 wt.% of Al_2O_3 is significantly lowered by the additional doping with Fe_2O_3 (Fig. 4c). Fe_2O_3 also retards the medium-term hydration reaction and lowers the maximal thermal power. This results in a very strong drop in cumulative heat of hydration during the first day. Like samples doped only with Fe_2O_3, the cumulative heat after 7 days is higher.

The effect of combined doping with MgO, Al_2O_3 and Fe_2O_3 is illustrated in Figs. 5–7. Again, the influence of MgO on the hydration characteristics is quite small and Al_2O_3 and Fe_2O_3 dominate the hydration characteristics of C_3S in the short-, medium-, and long-term.

Comparison of the hydration of doped C_3S with the structural data of C_3S [22] shows no direct correlation between the hydration and changes in the crystal structure caused by doping with foreign oxides. The best example for this is MgO. MgO causes the most visible changes in the crystal structure of C_3S and is, in addition, the only metal oxide that induces a conversion from triclinic to monoclinic. But, MgO has only a negligible influence on the hydration activity of C_3S. For Fe_2O_3 the situation is reversed. Structural changes detectable by XRD are insignificant, but the impact on the hydration is quite strong. Most likely this is because of the very complex hydration mechanism of C_3S which is not fully understood. An acceleration of C_3S hydration during the initial fast reaction can be interpreted as generation of active sites by the incorporation of foreign oxides. A hypothesis for the retardation mechanism is that specific foreign ions have a significant effect on the morphology of the layer of hydration products which are precipitated onto the grains of hydrated C_3S subsequent to the initial reaction. Due to changes in permeability, the diffusion of ions through the layer of hydration products into the solution and the diffusion of water in the opposite direction is altered.

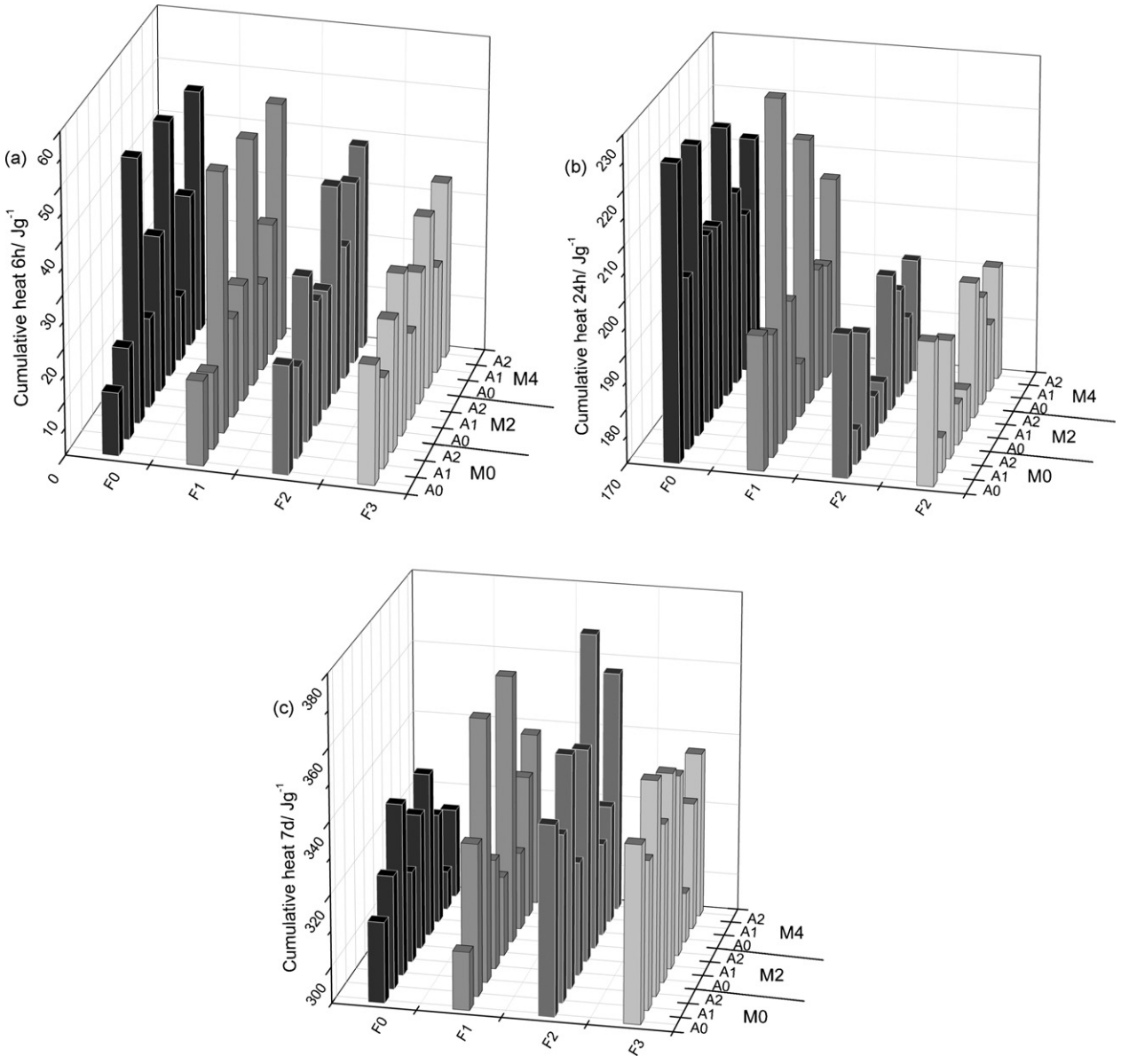

Fig. 6. Cumulative heat of hydration after 6 h, 1 day and 7 days.

3.4. X-ray diffraction patterns of hydration products

In Fig. 8 the XRD data of unhydrated and hydrated C_3S (90 days) are compared. In the hydrated samples, only traces of non-reacted C_3S are present. $Ca(OH)_2$ is the only product which is not X-ray amorphous and has by far the highest intensities in the XRD. The hydration products of C_3S either doped with Al_2O_3 or MgO did not show any differences compared to hydrated pure C_3S.

From diffraction data it can be summarised that Mg, Al or Fe do not form separate crystalline hydration products detectable by XRD, and foreign oxides which were incorporated into C_3S before the hydration are either incorporated into C–S–H phases or form amorphous products.

Table 2
Proportion of Q^n in wt.% of hydrated C_3S (90 days) measured by ^{29}Si MAS NMR

	Q^0 = unhydrated	Q^1	Q^2	Q^1/Q^2
C_3S pure	8.4	55.6	36.0	1.5
C_3S + 2.00% MgO	4.6	49.7	45.7	1.1
C_3S + 1.00% Al_2O_3	8.5	54.3	37.2	1.5
C_3S + 1.10% Fe_2O_3	9.5	59.0	31.5	1.9

3.5. DSC of hydration products

DSC of the hydrated samples shows the well-known trend—a continuous loss of water from C–S–H and a sharp peak around 470 °C caused by the decomposition of $Ca(OH)_2$. The characteristics of the graph and the quantified specific heat for the dehydration of $Ca(OH)_2$ was nearly the same for all samples, except for hydrated C_3S with high amounts of MgO. Fig. 9 shows that the sample containing 2 wt.% of MgO has an additional peak around 380 °C which was identified as decomposition of $Mg(OH)_2$. For this sample the specific heat for the decomposition of $Ca(OH)_2$ is about 18.5 J/g (~8%) lower than for the pure sample. For the interpretation we should bear in mind that during the hydration of C_3S about 50% of the calcium is bound to C–S–H and the other 50% forms $Ca(OH)_2$. In the sample with 2% MgO about 4% of the calcium is substituted by

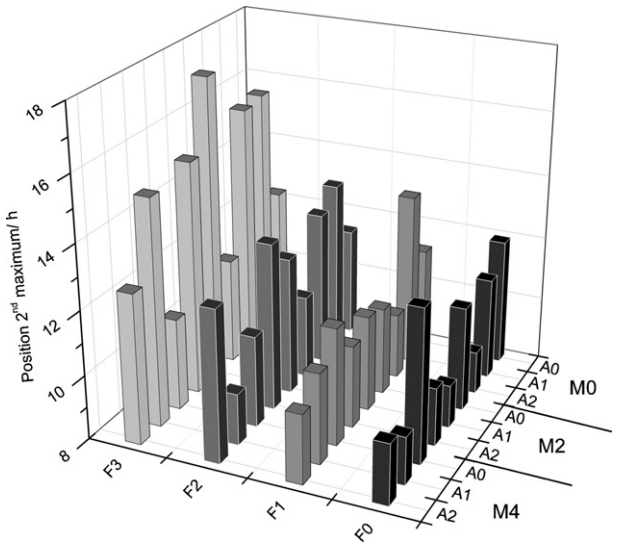

Fig. 7. Position of 2nd maximum.

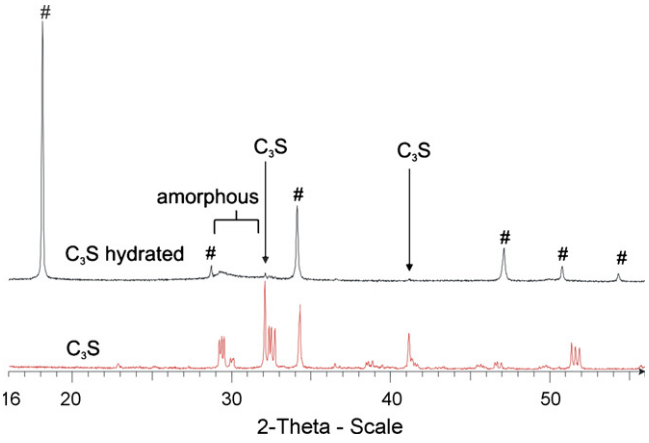

Fig. 8. XRD of unhydrated C_3S and C_3S hydrated for 90 days; #$Ca(OH)_2$.

magnesium. In this case the decrease in specific heat of ~8% means that not only 50% of the magnesium has formed X-ray amorphous $Mg(OH)_2$ but the bigger part of it.

3.6. ^{29}Si NMR of hydration products

By means of ^{29}Si solid-state NMR it is possible to detect all Si atoms in a sample quantitatively, regardless of whether the atoms are part of a crystalline or amorphous compound. Furthermore, different chemical shifts make it possible to distinguish between Si in the unhydrated C_3S (Q^0) and Si in C–S–H, where Si either bonds to one (Q^1) or more (Q^n, $n = 2, 3$) other Si atoms. In Fig. 10 the ^{29}Si NMR of unhydrated C_3S is compared with a sample hydrated for 7 days. Q^0 from Si bonds in C_3S is 34%, Q^1 is 48% and Q^2 is 18%, giving a ratio Q^1/Q^2 of 2.7. The results show that after 7 days about 1/3 of C_3S is unhydrated and that the degree of long C–S–H chains is low.

Fig. 11 shows the NMR spectra and Table 2 the proportion of Q^n of different samples hydrated for 90 days. The degree of hydration is >90% for all samples, but still some differences occur. The

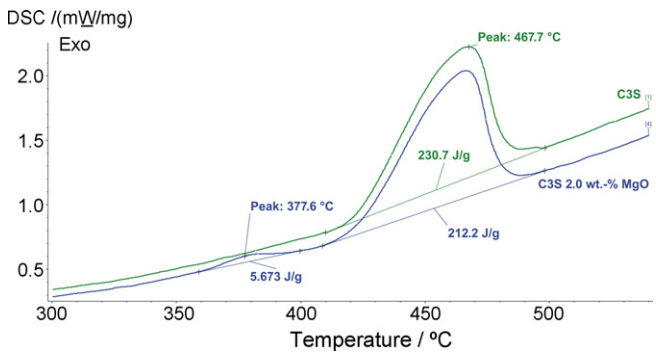

Fig. 9. DSC of 90 days hydrated pure C_3S and C_3S doped with 2.0 wt.% of MgO.

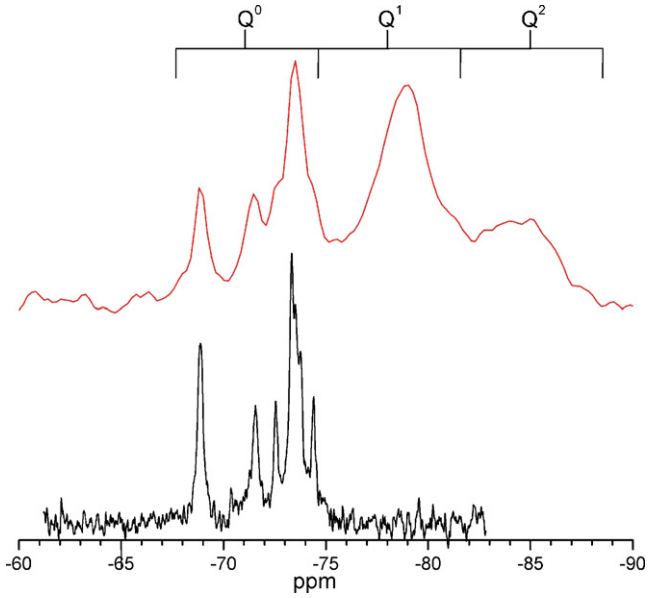

Fig. 10. ^{29}Si MAS NMR of pure C_3S (lower line) and C_3S hydrated for 7 days (upper line).

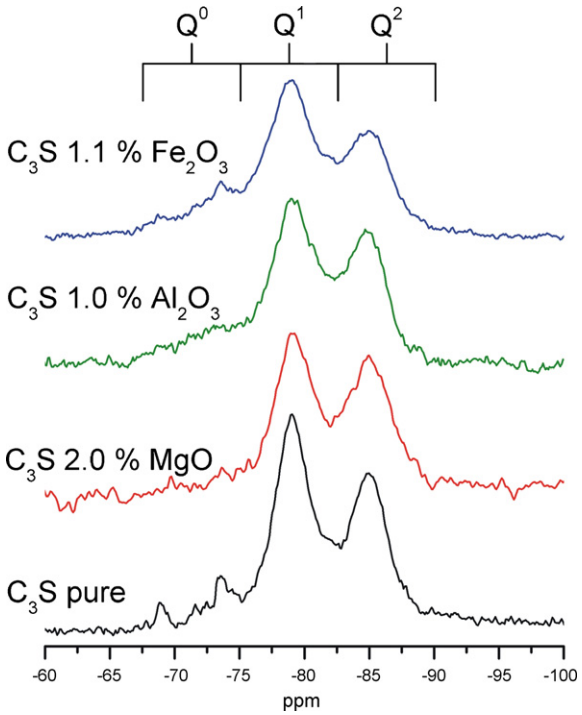

Fig. 11. ^{29}Si MAS NMR of pure C_3S and samples doped with MgO, Al_2O_3 or Fe_2O_3 hydrated for 90 days.

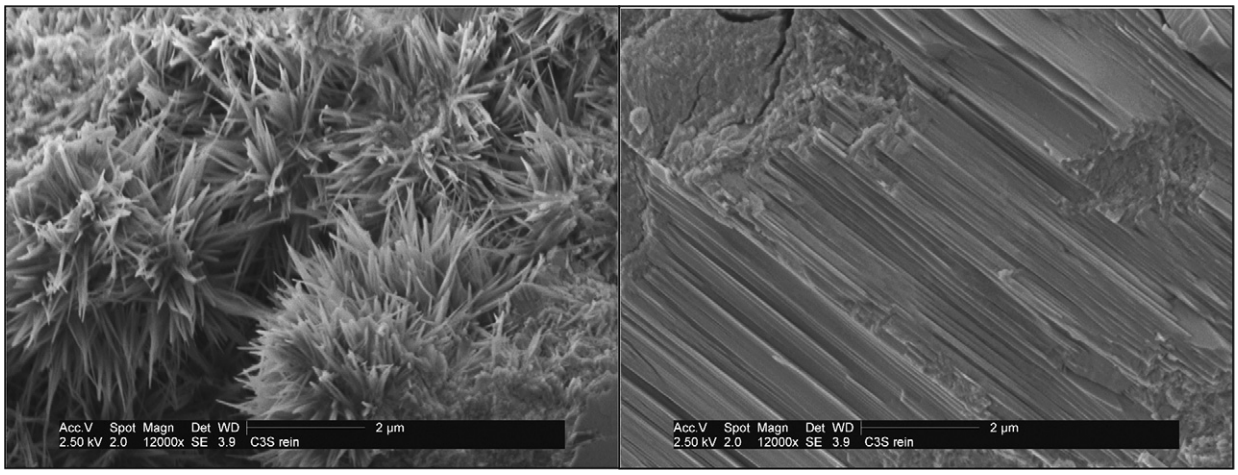

Fig. 12. SEM of pure C_3S, hydrated for 60 days; left: C–S–H; right: layered structure of portlandite.

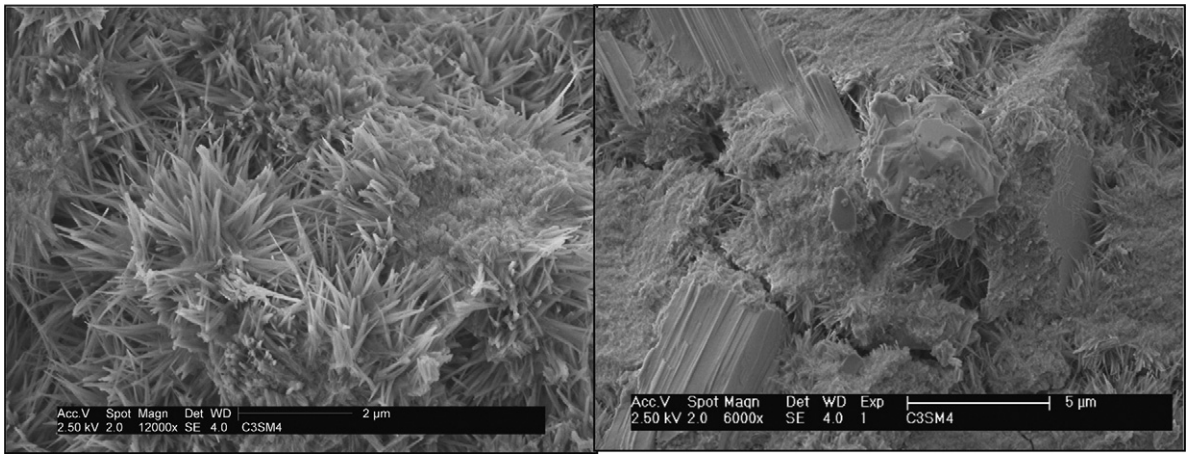

Fig. 13. SEM of pure C_3S with 2.0 wt.% MgO, hydrated for 60 days; left: C–S–H; right: layered structure of portlandite.

degree of hydration is highest for the sample doped with high amounts of MgO and lowest for the sample containing Fe_2O_3. For the sample without foreign oxides and the one containing high amounts of Al_2O_3 the ratio Q^1/Q^2 is equal, whereas it is higher for the sample with Fe_2O_3 and lower for the one containing MgO. These differences indicate that foreign ions not only alter the rate of hydration, but also the composition of the final product C–S–H.

3.7. Scanning electron microscopy of hydration products

In Figs. 12–15 the morphology of the hydration products of C_3S after 60 days of hydration is illustrated. On the one hand no differences appear between the hydration products of pure C_3S and the ones doped with MgO. C–S–H-phases form long and pointed needles and portlandite is crystallised in a well-ordered layered structure. On the other hand the appearance of samples containing

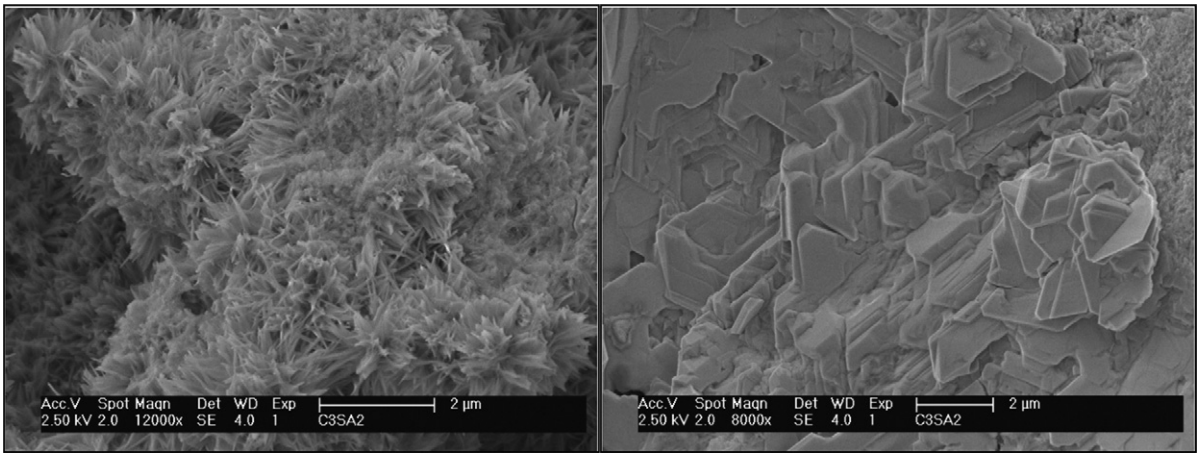

Fig. 14. SEM of C_3S with 1.0 wt.% of Al_2O_3 hydrated for 60 days; left: C–S–H; right: layered structure of portlandite.

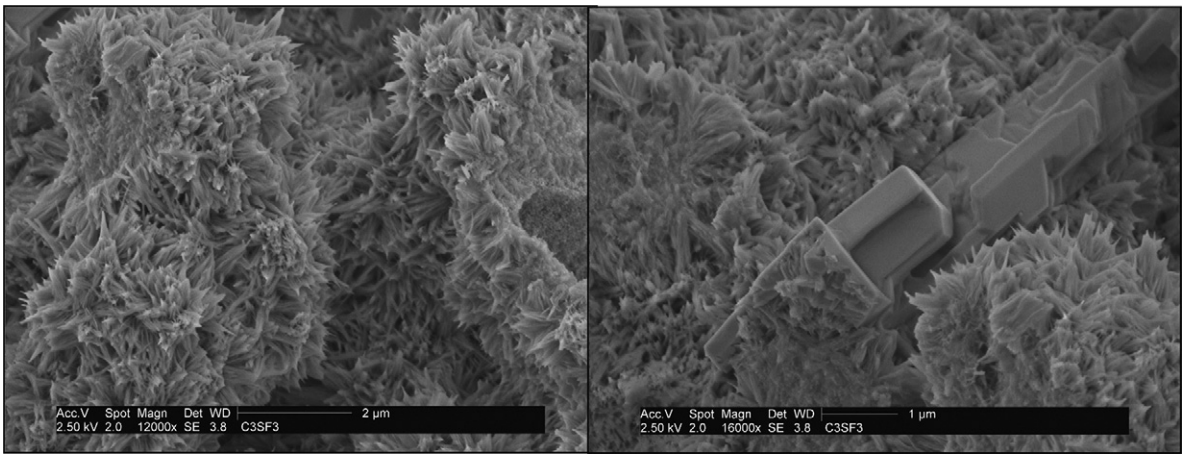

Fig. 15. SEM of pure C_3S with 1.1 wt.% of Fe_2O_3 hydrated for 60 days; left: C–S–H; right: layered structure of portlandite.

Al_2O_3 or Fe_2O_3 is comparable among each other, but different from the undoped sample. C–S–H-phases are shorter and more compact, whereas portlandite is crystallised in a less well-ordered structure. For quantitative conclusions more samples have to be investigated in detail, but again these differences clearly indicate changes in the morphology of the hydration products brought about by foreign ions.

4. Conclusion

The influence of single and multiple doping of tricalcium silicate with MgO, Al_2O_3 and Fe_2O_3 on the heat evolution during hydration is dominated by the kind and concentration of foreign oxides, and is independent of the influence of the doped oxides on the crystal structure. MgO has the least influence on the hydration during the first week, whereas Al_2O_3 especially accelerates the initial reaction and Fe_2O_3 broadens the main hydration reaction and decreases the maximum rate of heat evolution. For nearly all samples the cumulative heat of hydration after 1 week is higher for all doped samples than for undoped C_3S. If MgO is doped together with Al_2O_3 or Fe_2O_3 the hydration is dominated by Al_2O_3 or Fe_2O_3 and no interaction with MgO is detected. A combined doping of $Al_2O_3 + Fe_2O_3$ leads to an interaction of the doped oxides, whereas the strong initial reaction normally caused by high amounts of Al_2O_3 is prevented by Fe_2O_3 and the maximum of the main hydration peak is not only lowered but also retarded for several hours. After hydration the amount of $Ca(OH)_2$ in the MgO containing sample was lowered and some of the magnesium was detected as X-ray amorphous $Mg(OH)_2$ by DSC, the rest is incorporated into C–S–H or forms a separate X-ray amorphous compound. No indication is given for crystalline hydration products containing Al or Fe, therefore they are most likely incorporated into C–S–H. ^{29}Si NMR of samples hydrated for 90 days gives evidence of a lower degree of hydration for samples containing high amounts of Fe_2O_3. Samples containing high amounts of MgO have a higher degree of hydration and a higher proportion of Q^2. The results from SEM studies give evidence that the morphology of the hydration products from C_3S containing Al_2O_3 or Fe_2O_3 are different from the undoped or MgO containing C_3S. Compared to the usual appearance, the C–S–H-phases formed from C_3S containing Al_2O_3 or Fe_2O_3 are shorter and more compact, whereas portlandite is crystallised in a suboptimal ordered structure.

Acknowledgements

The authors thank the Deutsche Forschungsgemeinschaft for financial support. The authors are grateful to Prof. Dr. J. Plank for continuous support of the work.

References

[1] J. Bensted, P. Barnes, Structure and Performance of Cements, Spon Press, London, 2002.
[2] P.C. Hewlett, Lea's Chemistry of Cement and Concrete, Arnold, London, 1998.
[3] H.F.W. Taylor, Cement Chemistry, Academic Press, London, 1990.
[4] J. Plank, D. Stephan, C. Hirsch, in: R. Dittmeyer, W. Keim, G. Kreysa, K. Winnacker, L. Küchler (Eds.), Winnacker-Küchler: Chemische Technik, Wiley-VCH, Weinheim, 2004, pp. 1–167.
[5] D. Stephan, S. Wistuba, J. Eur. Ceram. Soc. 26 (2006) 141–148.
[6] D. Stephan, S. Wistuba, Cement Int. 3 (2005) 106–117.
[7] D. Stephan, S. Wistuba, Cem. Concr. Res. 36 (2006) 2011–2020.
[8] M.I. Alemany, P. Velasquez, M.A. de la Casa-Lillo, P.N. De Aza, J. Non-Cryst. Solids 351 (2005) 1716–1726.
[9] P.N. De Aza, Z.B. Luklinska, M.R. Anseau, F. Guitian, S. De Aza, J. Dent. 27 (1999) 107–113.
[10] Z. Gou, J. Chang, J. Eur. Ceram. Soc. 24 (2003) 93–99.
[11] Z. Gou, J. Chang, W. Zhai, J. Eur. Ceram. Soc. 25 (2005) 1507–1514.
[12] W. Zhao, J. Chang, J. Biomed. Mater. Res. A 73 (2005) 86–89.
[13] W. Zhao, J. Chang, Mater. Lett. 58 (2004) 2350–2353.
[14] F.W. Locher, ZKG Int. (1967) 402–407.
[15] K. Garbev, Naturwissenschaftlich-Mathematische Gesamtfakultät, Ruprecht-Karls-Universität, Heidelberg, 2004, pp. 271.
[16] E.M. Gartner, J.F. Young, D.A. Damidot, I. Jawed, in: J. Bensted, P. Barnes (Eds.), Structure and Performance of Cements, Spon Press, London, 2002, pp. 57–113.
[17] I. Odler, in: P.C. Hewlett (Ed.), Lea's Chemistry of Cement and Concrete, Arnold, London, 1998, pp. 241–297.
[18] J. Skibsted, C. Hall, H.J. Jakobsen, in: J. Bensted, P. Barnes (Eds.), Structure and Performance of Cements, Spon Press, London, 2002, pp. 457–477.
[19] I.G. Richardson, G.W. Groves, J. Mater. Sci. 32 (1997) 4793–4802.
[20] M.D. Andersen, H.J. Jakobsen, J. Skibsted, Inorg. Chem. 42 (2003) 2280–2287.
[21] D. Stephan, P. Wilhelm, Z. Anorg. Allg. Chem. 630 (2004) 1477–1483.
[22] D. Stephan, S.N. Dikoundou, G. Raudaschl-Sieber, Mater. Struct. (2008), doi:10.1617/s11527-11008-19360-11523.
[23] S. Abdul-Maula, I. Odler, Br. Ceram. Proc. 35 (1984) 83–91.
[24] G.L. Valenti, V. Sabatelli, B. Marchese, Cem. Concr. Res. 8 (1978) 61–72.
[25] P. Fierens, M. Thauvoye, J.P. Verhaegen, Influence of Iron(III) and Titanium(IV) on the Structure and Reactivity of Tricalcium Silicate, vol. 69, 1972, pp. 211–222.